Contents lists available at http://qu.edu.iq

Al-Qadisiyah Journal for Engineering Sciences

Journal homepage: https://qjes.qu.edu.iq

Theoretical model to predict the flexural response of concrete beams pre-tensioned with CFRP rods considering CFRP slippage effects

Yasir M. Saeed [1,2]*, ***Karrar Al-Lami*** [3], ***and Franz Rad*** [4]

[1]*Directorate of Research and Development, the Ministry of Higher Education and Scientific Research, Iraq*
[2]*Department of Civil Engineering, College of Engineering, Tikrit University, Tikrit, Salah Al-Deen, Iraq.*
[3]*Civil Engineering Department, College of Engineering, University of Wasit, Al-Kut, Wasit, Iraq.*
[4]*Department of Civil and Environmental Engineering, College of Engineering and Computer Science, Portland State University, P.O. Box 751, Portland, Oregon 97207, USA*

ARTICLE INFO

Article history:
Received 01 May 2024
Received in revised form 01 July 2024
Accepted

Keywords:
Bond
CFRP
Flexural performance
Prestressed concrete beams
Pre-tension
Slippage
Theoretical analysis

ABSTRACT

The overwhelming costs of maintenance for reinforced concrete structures due to steel corrosion have motivated researchers to look for alternatives. One of the promising alternatives is Fiber Reinforced Polymer (FRP). Among FRP materials, Carbon FRP (CFRP) is the most attractive material for prestressed concrete members due to its high tensile strength and modulus of elasticity. Previous studies investigated the use of CFRP in prestressed concrete through experimental tests and theoretical analysis. However, there is a significant need for more experimental data to develop an accurate model that can accurately predict the behavior of CFRP prestressed concrete beams. In the current study, experimental flexural tests were conducted on four prestressed concrete beams pre-tensioned with CFRP rods. The length of the beams was 4,270 mm, and the cross-sectional dimensions were 138 x 250 mm. All the beams were subjected to four-point loading with an initial five cycles of loading and unloading before a monotonic loading until failure. Their performance was analyzed, and based on the results a theoretical model was proposed. It was found that the slippage of CFRP at the ends significantly affect the flexural behavior and failure modes of the beams. Additionally, theoretical models must account for CFRP slippage at the ends to accurately predict the flexural response of CFRP prestressed concrete beams. When a slippage reduction factor was used in the proposed theoretical model, the results had a good agreement with the experimental tests. Future research may focus on testing the theoretical model with more data from experimental studies.

1. Introduction

Here The use of advanced materials, like FRP materials, in structural engineering has become more needed for more durable and efficient structures. For prestressed concrete members, Carbon fiber reinforced materials (CFRPs) are the most desirable type as it has the strongest tensile capacity associated with high modulus of elasticity. In addition, CFRP materials are known for their high resistance to corrosion and low weight, which make CFRPs interesting alternative materials for reinforced and prestressed concrete [1–3]. CFRP material can address some of the concerns with steel bars related to durability. Since CFRP rods have an exceptional corrosion resistance, the durability of concrete structures

* *Corresponding author.*
E-mail address: yasirmsaeed@gmail.com (Yasir M. Saeed)

https://doi.org/10.30772/qjes.2024.152275.1326

reinforced or prestressed with CFRP rods is much higher especially considering concrete structures that are subjected to harsh environment [4–6]. Moreover, the low weight of CFRP enables the possibility of longer structural members, which is significant for prestressed concrete design [7–9]. The use of CFRP in prestressed concrete members have been studied extensively by several researchers to investigate the possibility of using CFRP rods as an alternative for steel strands [10–15]. The studies by Saadatmanesh and Ehsani [16] and Malek et al. [17] and Braimah et al. [18] were some the pioneer studies that stated the feasibility of using CFRP rods in prestressed concrete elements. They reported that CFRP rods had significant features that could enhance the flexural performance and stiffness of prestressed concrete beams. In addition, they show that using CFRP could the overall cost of the structures due to the light weight of CFRP compared to steel and the maintenance required for concrete structures reinforced with steel. The possibility of predicting the flexural response of CFRP-prestressed concrete members is the key to increase the confidence of using CFRP in prestressed concrete members. Therefore, it is essential to propose theoretical or numerical models that can predict the performance of prestressed concrete beams with CFRP rods. There were a number of studies that proposed theoretical predictions of the flexural performance of concrete beams prestressed with CFRP materials [19–22]. Their results motivated researchers to conduct further studies on the use of CFRP in prestressed concrete members. One of the great challenges in predicting the performance of concrete beams prestressed with CFRP materials is the FRP-to-concrete bond properties. Unlike reinforced concrete members, the idea of prestressing CFRP increases the challenge of fully understand the bond characteristics between CFRP and concrete because in prestressed concrete elements the prestressing force would transfer from CFRP to concrete section through the bond between the two materials. This suggests a significant need to develop a model that can accurately predict the flexural performance of CFRP prestressed concrete beams using available experimental data. In the current study, four CFRP prestressed concrete beams were tested under flexural loading to better understand their behavior. Then, a simple theoretical model was proposed that can easily be used to calculate the flexural capacity of CFRP prestressed concrete members. Since bonding is the most critical challenge in terms of predicting the flexural behavior of prestressed concrete beams with CFRP rods, the model used the experimental data to propose a reduction factor to account for the CFRP slippage at the ends. The results of this paper can be used for future studies to fully understand the behavior of prestressed concrete elements prestressed with CFRP and accurately predict their response.

2. Materials properties

2.1. CFRP rods

In this study, a 12.7 mm diameter CFRP rods were used. The CFRP rods were sand coated and had helical wrap. Based on the datasheet from the manufacturer, the maximum tensile strength, strain, and modulus of elasticity are 2068 MPa, 0.0167, 124 GPa, respectively. However, the maximum tensile strength, strain, and modulus of elasticity of the CFRP rods based on the four ASTM specimens [23] tested in the laboratory were 2282 MPa, 0.0162, and 141 GPa, respectively. Fig. 1 shows the stress-strain relationships for the tested CFRP rods compared to the manufacturer data. It can be seen that at about 70% of the maximum load, the extensometer was removed. Therefore, no strain data could be obtained after that.

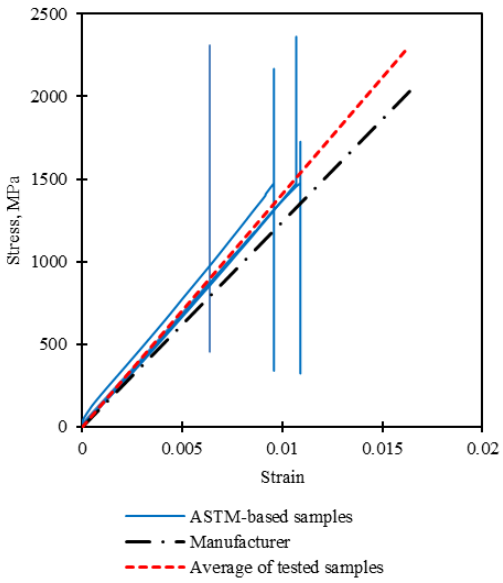

Figure 1. Stress-strain relationship for CFRP rods

2.2. Concrete

The concrete mixture was designed based on "Designing and Proportioning Normal Concrete Mixtures" by Portland Cement Association (2002) to achieve a nominal concrete strength of 50 MPa. Three cylinders for each beam specimen were tested to determine the compressive strength of the concrete for each beam. The results showed that the compressive strength for the four beams were 50, 53, 50, 52 MPa for B1 (Beam no. 1), B2, B3, B4, respectively. In addition, three other cylinders were tested to determine the modulus of elasticity and the stress-strain relationship (based on ASTM C469 [24]) as they would be needed for the theoretical model. The modulus of elasticity for B1, B2, B3, and B4 were 41, 42, 41, and 42 GPa, respectively. The results of the stress-strain relationships will be discussed later in this paper as part of the theoretical model.

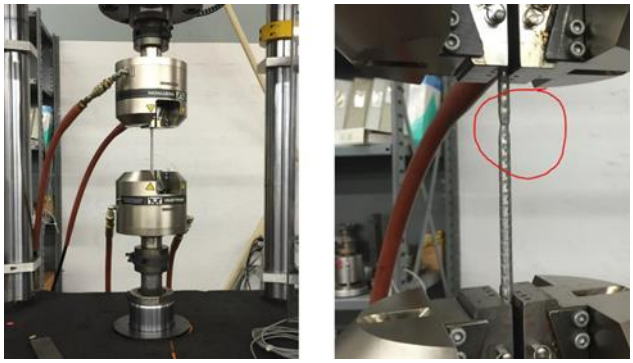

Figure 2. Test setup for steel bars used for stirrups (D5)

2.3. Steel wires

Deformed steel wires commercially known as D5 were used for shear reinforcement. The diameter of D5 is 6.35 mm. Based on the manufacturer datasheet, the breaking capacity of D5 is 752 MPa. Two samples were tested in the laboratory (Fig. 2), and the average maximum achieved tensile capacity was 689 MPa. The stress-strain relationships are presented in Fig. 3. It can be seen that there is no clear yielding strength for D5, but it can be estimated to be 480 MPa. For design purposes, the yield strength of D5 was assumed to be 400 MPa.

It must be mentioned that typically three samples should be tested to determine an experimental value. However, all what the authors needed from testing the steel wires in the current study was to determine the tensile strength of the steel wire. The results of the two specimens showed that the breaking strength was around 689 MPa, and the design value was 400 MPa. Therefore, testing another sample wouldn't have made any difference.

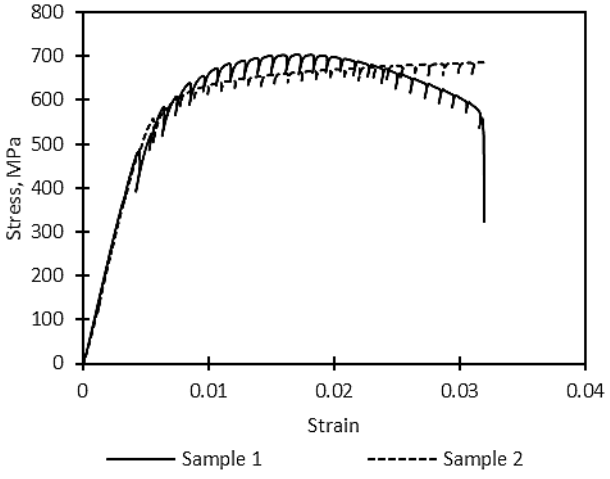

Figure 3. Stress-strain relationship for steel wires D5

3. Flexural tests

3.1. Beam design

Four large-scale concrete beams pre-tensioned with CFRP rods were experimentally tested in the current study. The total length of the beams was 4270 mm, with a clear span of 4110 mm. The cross-sectional dimensions were 138 mm x 250 mm. The beams were pre-tensioned with one CFRP rod, the eccentricity of which equal to 89 mm, resulting in a prestressing reinforcement ratio of 0.0042. The beam specimens were designed to have a prestressing reinforcement ration slightly higher than the balanced ratio, and the failure is expected to be concrete crushing in the compression zone, which is desirable to avoid CFRP rupture [25]. As mentioned earlier, D5 steel wires were used for shear reinforcement and the design was based on the minimum shear reinforcement provided by ACI 318 [26]. For B1 (Beam 1), stirrups' spacings of 150 mm (center-to-center) were used. However, it was found that due to CFRP slippage during the flexural tests, more shear reinforcement was required. Therefore, stirrups' spacing of 75 mm was used along the shear span of the other beam specimens. The problem with shear was only due to excessive CFRP slippage at the ends which reduced the upward force due to prestressing and caused the failure. This issue was partially solved in B2 and B3 by increasing the shear stirrups, which consequently increased the bond between CFRP and concrete. The idea of increasing shear reinforcement increases the confinement, improves the bond, and reduces the development length has been reported and proved by several researchers [27–29].

To eliminate the slippage effects on the behavior of the beams, CFRP rod was locked at the end for Beam 4 (B4). The novel anchorage system developed by Saeed et al. [30] was used to lock the CFRP rods at the beam ends and to prevent any slippage and losses in the prestressing force. Fig. 4 shows the difference between the beam ends for B4 compared with the other beam specimens.

Figure 4. The differences in beam ends for B4 and the other three beam specimens

Table 1. Prestressing data for CFRP prestressed concrete beam specimens

Beam Specimen	*B1*	*B2*	*B3*	*B4*
Nominal prestress level	65%	55%	60%	60%
Jacking stress (MPa)	1340	1140	1240	1280
Initial stress, f_{pi}, after transfer (MPa)	1220	1080	1130	1195
Immediate losses (%)	3.8	3.7	4.7	4.9
Effective stress, f_{pe}, (MPa)	1230	1080	1120	1200
Total losses (%)	8.7	4.8	9.4	6.6
Initial concrete compressive strength, f'_{ci} , (MPa)	45	48	47	51
Concrete compressive strength, f'_c , (MPa)	50	53	50	52

3.2. Instrumentations and loading

During the pre-tensioning process, the jacking force was monitored and recorded using a hollow load cell attached to the hydraulic ram used to apply the tension force and pull the CFRP rod. In addition, eleven strain gauges were attached to the surface of CFRP rod to accurately measure the strain during the pre-tensioning process, releasing process, and during the flexural tests of the beam. Once the CFRP rod is pre-tensioned to the designed jacking force (Table 1), concrete was cast and let to cure for two weeks. The next step was to release the jacking force. The jacking force was released slowly and carefully, and the data of releasing the force were recorded as can be seen in Table 1. Twenty-one days after casting the concrete, the beam specimens would be prepared for flexural testing. One Linear Variable Differential Transformers (LVDT) was used to measure the beam deflection at mid-span, and two LVDTs were used to measure the end slippage of CFRP rod. All instrumentations were connected to a data logging system to monitor, record, and store the data simultaneously from the load cell, LVDTs, and strain gauges. Fig. 5 shows the test setup and instrumentation for the flexural test. Five cycles of loading were applied to each beam before a monotonic loading until failure. The load for the first five cycles was equal to 65% of the maximum estimated strength (the maximum flexural strength calculated theoretically based on the mechanical properties of concrete and CFRP rod) or when the tensile CFRP strain reached 0.01. Then the load was applied monotonically until failure.

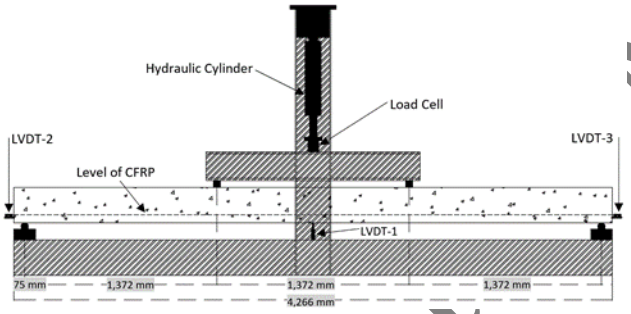

Figure 5. Test setup for beam specimens

4. Experimental results and discussions

4.1. Moment-deflection relationship

Figure 6 shows the moment-deflection curves for the four beam specimens. Overall, the moment deflection curves for all tested beams were almost bilinear. Up until the cracking moment, the behavior of the prestressed beams was linear. Then after the cracking moment, the behavior was almost linear but with a much lower stiffness. The first three beams experienced CFRP slippage at the ends leading to lower post-cracking stiffness compared to B4. It was observed that all beams experienced a permanent deflection after the five cycles of loading. Specimen B1 failed unexpectedly due to the extensive CFRP slippage at the ends. It could only handle 39 kN-m before it failed brittlely with a shear failure mode. B2 had the same failure mode but with 22% improvement in maximum strength and a much better ductility due to the enhancement of shear reinforcement at the ends. The performance of specimen B3 was similar to B2 with a slightly lower moment capacity but larger ultimate deflection. A significant improvement was observed in specimen B4 in terms of maximum moment capacity, post cracking stiffness, failure mode, and deformability. The maximum moment capacity was 62% higher than B1 and 34% higher than B2. Moreover, the failure mode was concrete crush at the compression zone as it was designed. Locking CFRP at the ends prevented the CFRP slippage, which led to utilizing most of the CFRP strength and improved the flexural capacity of the beams.

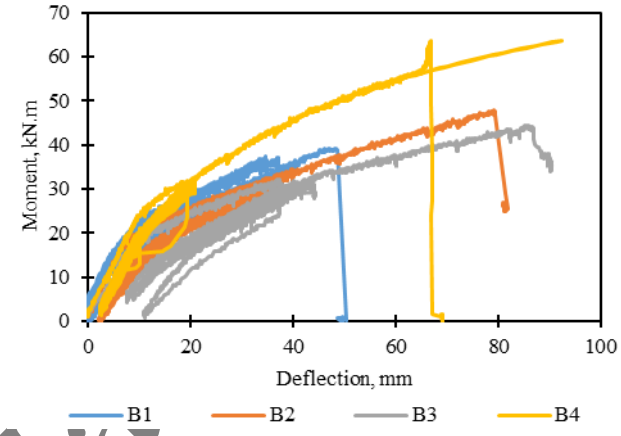

Figure 6. Moment-deflection curves for beam specimens

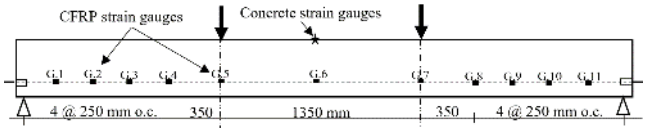

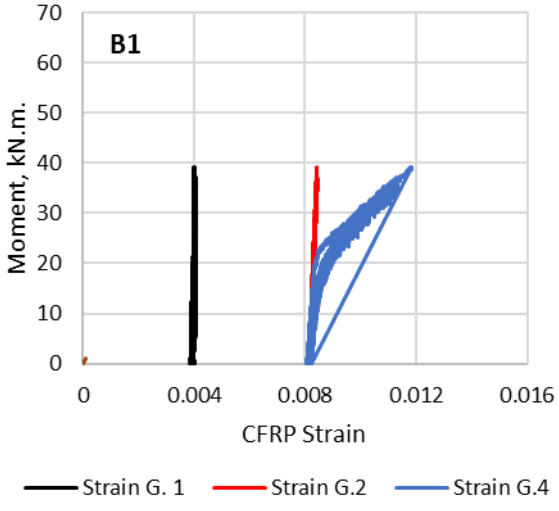

Figure 7. Moment vs. CFRP tensile strain relationship during the flexural test

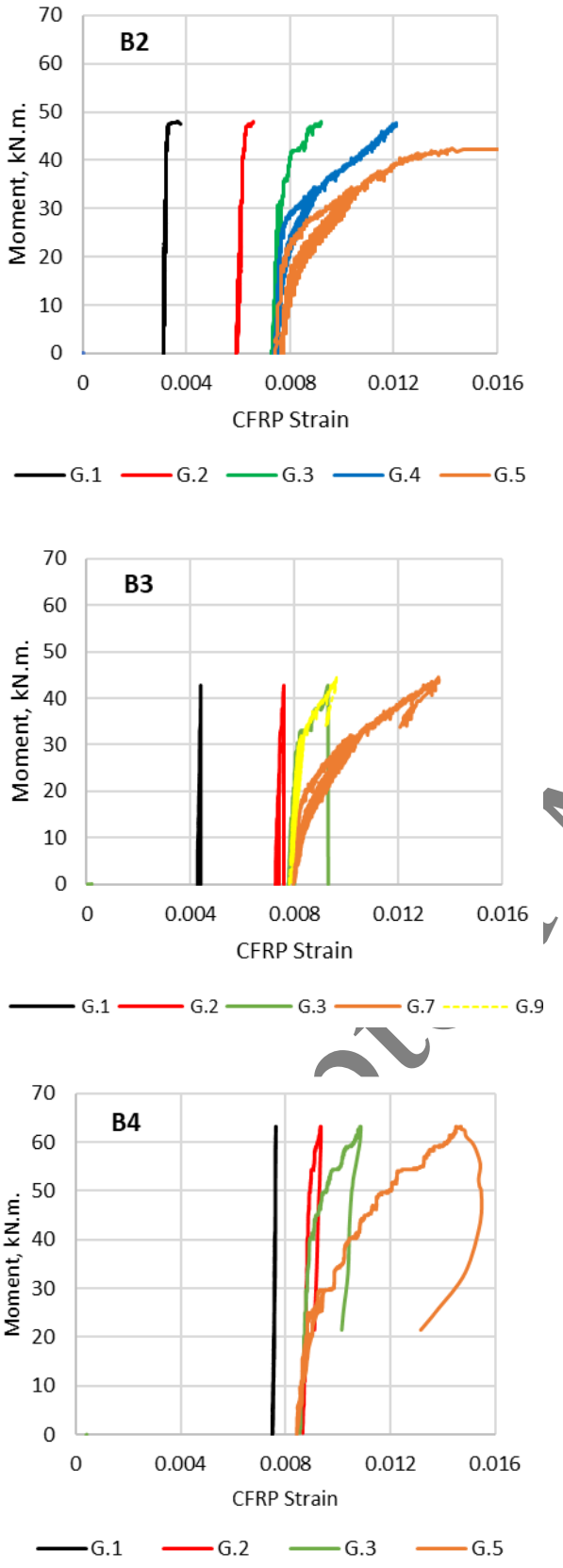

Figure 7. Moment vs. CFRP tensile strain relationship during the flexural test (***continued***)

Figure 7 shows the moment - CFRP tensile strain relationship for the four beam specimens. It can be seen that CFRP strain in the shear span for B1 did not record any strain during the test. This could be strain gauge failure (detachment) or due to slippage. It should also be mentioned that the data from most of the strain gauges were lost during the prestressing and load transfer. For B2, it can be noticed that small strains were recorded by G.1 and G.2 when the load approached the maximum. Strain gauge G.3 recorded increase in CFRP strain when the load was beyond 30 kN.m. Similar observation was found for B3 specimen where the CFRP strain increased when the load exceeded 30 kN.m (see the readings of G.3 and G.9 for B3 specimen). Regarding B4, it was the only specimen to see an increase in CFRP strain at G.2 location. This was mainly because of preventing the CFRP slippage at the ends using the anchorage system in B4.

4.2. Deformability

For FRP reinforced or prestressed concrete members, the terminology "deformability" is used instead of ductility because FRPs do not yield [31]. It is still controversial about how to evaluate the ductility or deformability of concrete members reinforced with FRPs. Abdelrahman et al. [32] proposed that the deformability of the member can be determined by dividing the actual maximum deflection by an imaginary deflection corresponding to the maximum load assuming un-cracked section of the concrete beam. On the other hand, Zou [33] stated that the deformability of FRP prestressed concrete beams could be determined by dividing the maximum moment by the cracking moment and multiply the result by the maximum deflection divided by the cracking deflection. The deformability of the beams was evaluated and the results are shown in Table 2. It can be seen that B2 and B4 had the best performances in terms of deformability. The current controversy around deformability evaluation methods indicates a need for standardized guidelines. It is highly desirable to establish standard guidelines in the near future.

Table 2. Deformability of CFRP prestressed concrete beams

Beam Specimen	***B1***	***B2***	***B3***	***B4***
M_{cr} *(kN.m.)*	24	19	19	26
Δ_{cr} *(mm)*	14	10	12	11
$M_{max.}$ *(kN.m.)*	39	47	45	64
$\Delta_{max.}$ *(mm)*	48	79	86	92
Deformability based on Abdelrahman et al. [32]	2.53	4.00	3.78	3.82
Deformability based on Zou [33]	5.55	20.70	16.79	20.41

5. Theoretical model

The theoretical model was developed to predict the moment-deflection relationship of CFRP prestressed concrete beams. The model depends on a very basic mechanics of materials and strain compatibility. Since the stress-strain behavior of each material used in the concrete beam was determined experimentally and known, then strain compatibility could be applied to determine the moment deflection relationship for the beam as a composite

element. The following sections will explain the assumptions, materials properties, the analysis, and the results.

5.1. Assumptions

The key principle used in the analytical model was strain compatibility. It was assumed that in the first stage of the analysis, which was before the cracking moment, the beam behaved elastically without cracks. Therefore, the force at the bottom of the concrete section resulted from the concrete material below the neutral axis and the CFRP rod. The area of CFRP material was converted to concrete based on the modulus of elasticity of each material. Basic mechanics of material principles were used to determine the deflection at this stage. The upward deflection would result from the CFRP force and the downward deflection from the applied load [34]. The plastic analysis started after reaching the cracking moment. At this stage, only the CFRP force was considered below the neutral axis, and the concrete contribution in the tension zone was ignored. The analysis solely deepened on the stress-strain relationship of CFRP material in the tension and the concrete stress-strain relationship in the compression. The beam was assumed to fail if CFRP stress reached the ultimate (2,282 MPa as defined in section 2.1 of this study) or when concrete strain reached 0.003. Perfect CFRP-to-concrete bonding was assumed.

5.2. Materials properties

The stress-strain relationship for CFRP rods presented in Fig. 1 was used for the theoretical analysis. For the concrete, the stress strain relationship used in the theoretical model was a mix between the experimental results and the equation originally proposed by Hognestad in 1951 [35]. The equation was manipulated to represent almost the same stress-strain relationship obtained from the experimental tests. It is worth mentioning that the stress-strain curve was different if the creep effect was considered in the cylinder test. As it is known, the flexural tests of the beam specimens took between 90 to 120 minutes.

least 90 minutes before failureThe effects of creep (tests that lasted for 90 minutes) can clearly be seen in Fig. 8. The stress-strain relationship of concrete considering creep was then used in the theoretical model. The terminology “Theoretical-1” in Fig. 8 represent the theoretical representation of the short-time test. For Theoretical-1, the concrete strain associated with the maximum concrete stress was fixed to 0.002 as suggested by Hognestad [35]. However, for Theoretical-2 the concrete strain associated with the maximum concrete stress was taken from the experimental results, and it was different for each beam as shown in Fig. 8.

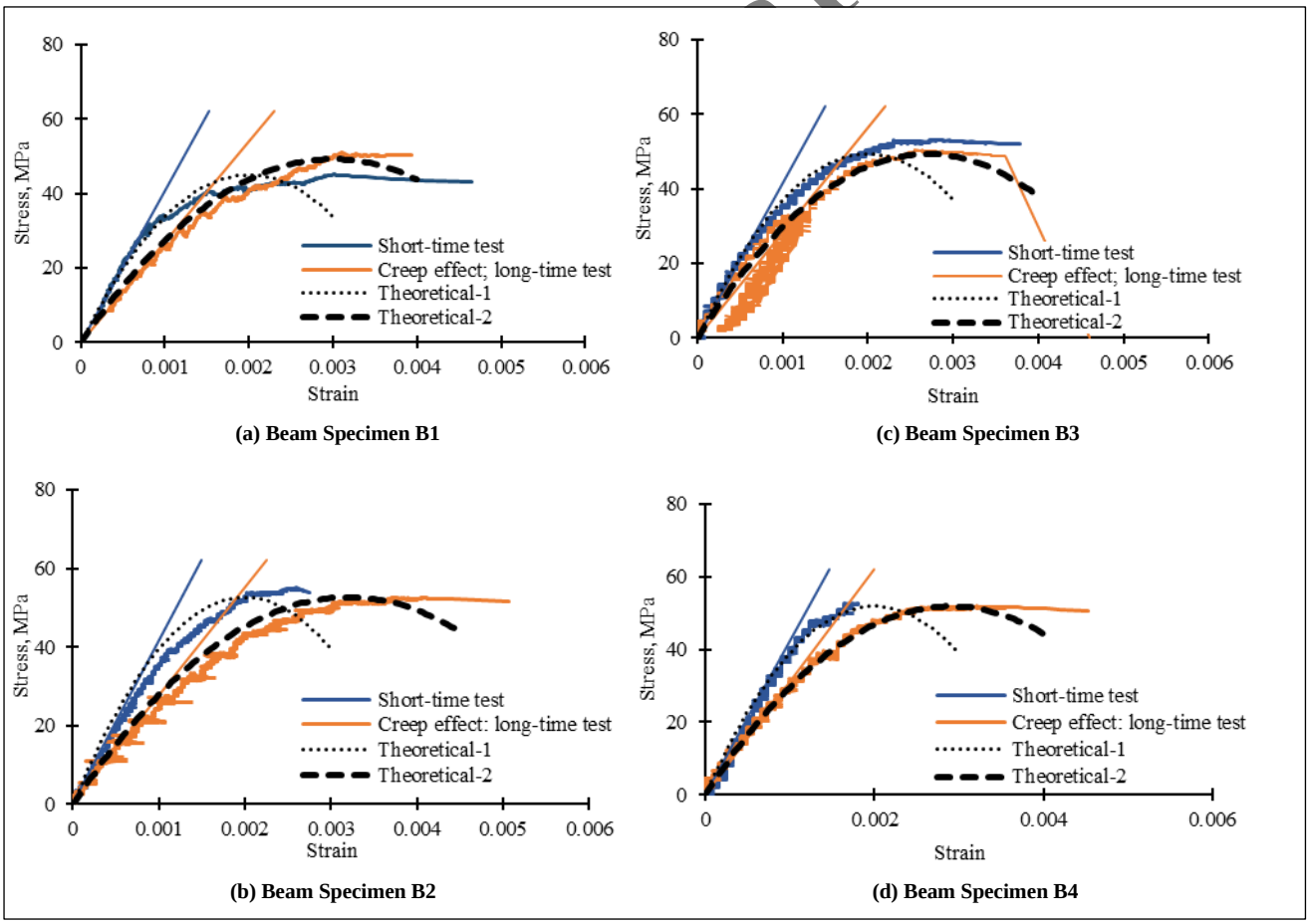

Figure. 8 Stress-strain relationship for concrete material considering the creep effect; Theoretical-1 represents the theoretical simulation of the short-time test, and Theoretical-2 represents the theoretical simulation of the long-time test considering the creep effect

1.1. Theoretical analysis

The stress The analysis mainly depended on the guidelines proposed by ACI 440 [25,36] and the following references [34,37,38] in addition to basic mechanics of materials. MATLAB software [39] was utilized to compute the flexural response of CFRP prestressed concrete beams depending on the stress-strain relationships of the individual components and depending on the level of prestress. The model used an iterative approach by constantly changing the assumption of the concrete strain at the maximum fiber of concrete section and the location of the neutral axis until the tension force below the neutral axis became equal to the compression force above the neutral axis. In the beginning of the analysis, the applied load was assumed to be zero, ignoring the beam's own weight. This is in agreement with the analysis of the experimental results because the presented experimental moment-deflection relationships did not account for self-weights. In this stage of analysis, the model only counts for the upward moment from the prestressing force:

$$\sigma_{top} = -\frac{P_{fe}}{A} + \frac{P_{fe} \cdot e \cdot c}{I} \quad (1)$$

$$\sigma_{bottom} = -\frac{P_{fe}}{A} - \frac{P_{fe} \cdot e \cdot c}{I} \quad (2)$$

Where;

σ_{top} = concrete top fiber stress, MPa
σ_{bottom} = concrete bottom fiber stress, MPa
P_{fe} = effective CFRP pre-tensioning force, N
A = area of the beam's cross section, mm^2
e = CFRP eccentricity, mm
c is the distance from the central axis to the specific point where stress is being measured, mm
$I = \frac{b\,h^3}{12}$, mm^4

The strains will then be calculated based on the concrete stresses at the top and bottom fibers using the stress strain relationship of the concrete. Then, the curvature (φ_0) was determined using the geometry of the cross-section, as shown in equation 3 and explained in Fig. 9:

$$\varphi_0 = \frac{\varepsilon_{bot} - \varepsilon_{top}}{h} \quad (3)$$

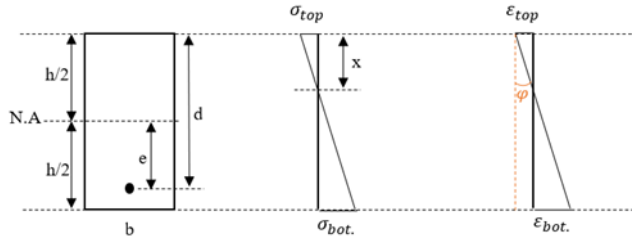

Figure 9. Explanation of the concrete cross-sectional stresses and strains

Equation 3 represents the curvature of the cross-section when the load is zero. Then, Equations 1 and 2 could be used to determine the strain at concrete at the level of CFRP rod (ε_{ce}).

$$\sigma_{ce} = -\frac{P_{fe}}{A} + \frac{P_{fe} \cdot e \cdot e}{I} \quad (4a)$$

$$\varepsilon_{ce} = \frac{\sigma_{ce}}{E_c} \quad (4b)$$

The next step was to determine the strain value at the very bottom of the cross-section corresponding to modulus of rupture. This would lead to determining the cracking moment. Another point on the moment curvature relationship was found when the concrete stresses at CFRP level was zero. Therefore, the CFRP strain at this stage was the effective strain due to pre-tensioning in addition to ε_{ce}. After that the new curvature point (φ_1) can be determined using Equation 3.

$$P_{f,1} = P_{fe} + \sigma_{ce} * A_b \quad (5)$$

$$M_1 = \frac{I\,\sigma_{ce}}{e} \quad (6)$$

$$\sigma_{top1} = -\frac{P_{f1}}{A} + \frac{P_{f1} \cdot e \cdot c}{I} - \frac{M_1 \cdot c}{I} \quad (7a)$$

$$\sigma_{bot.1} = -\frac{P_{f1}}{A} - \frac{P_{f1} \cdot e \cdot c}{I} + \frac{M_1 \cdot c}{I} \quad (7b)$$

Now, the cracking stress ($0.62\sqrt{f_c'}$, MPa) was the bottom stress from Equation (7b) plus the extra stresses causing the cracks. These additional stresses would cause additional moments. Therefore, to determine the cracking moment, the moment when the stresses at CFRP level was zero could be added to the additional moment caused by the additional stresses causing the cracking, as explained by the equations below:

$$f_{cr} = 0.62\sqrt{f_c'} \quad \text{ACI 318 [26]}$$

$$\Delta f = f_{cr} - \sigma_{bot.1} \quad \text{so,} \quad \Delta M = \frac{\Delta f \,.\, I}{c} \quad (8)$$

$$M_{cr} = M_1 + \Delta M \quad (9)$$

$$\Delta f_{fp} = \frac{\Delta M \,.\, e \,.\, n}{I} \quad (10)$$

$$P_{f,cr} = P_{f,1} + \Delta f_{fp}\,(A_b) \quad (11)$$

$$\sigma_{top2} = -\frac{P_{f,cr}}{A} + \frac{P_2 \cdot e \cdot c}{I} - \frac{M_2 \cdot c}{I} \quad (12a)$$

$$\sigma_{bot.2} = -\frac{P_{f,cr}}{A} - \frac{P_{f,cr} \cdot e \cdot c}{I} + \frac{M_{cr} \cdot c}{I} \quad (12b)$$

After that the new curvature point corresponding to cracking moment could be determined using Equation 3. After this point, plastic analysis was applied as the beam had passed its elastic point. At this stage, the concrete force in tension was neglected (Fig. 10). Below the neutral axis, the source of the tension force was from CFRP rods only. Using the stress-stain relationship of CFRP material (Fig. 1), the CFRP force below the neutral axis was determined. Similarly, the compression force above the neutral axis was determined using concrete's stress-strain curve:

$$C = b.f_c'.\frac{\varepsilon_c}{\varepsilon_o}.x.\left[1 - \frac{\varepsilon_c}{3.\varepsilon_o}\right] \quad (13)$$

$$y' = x.\left[\frac{8.\varepsilon_o - 3.\varepsilon_c}{12.\varepsilon_o - 4.\varepsilon_c}\right] \quad (14)$$

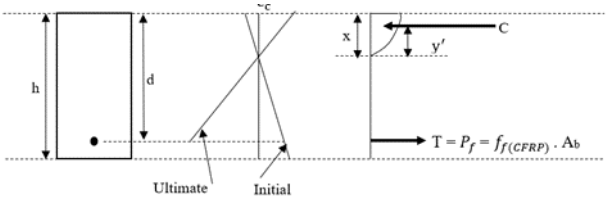

Figure 10. Cross-sectional analysis of the concrete beam showing the compression and tension forces

The next step was a trial and error method. The top fiber concrete strain and the location of neutral axis (c) were assumed, and based on which the tension and compression forces were calculated. The assumed location of neutral axis would be considered correct if the tension and compression forces were in equilibrium. If not, a different location of the neutral axis would be assumed until reaching the equilibrium, which means that the assumed concrete strain and the location of the neutral axis were correct. The process continued until the full curve of moment-curvature was developed. From the moment-curvature relationship, moment vs. mid-span deflection curves can be developed by applying the second moment-area theorem (Fig. 11). For example, the deflection corresponding to M_{cr} was determined by multiplying $Area_1$ by the distance from the center of the area to point A. For maximum deflection, or the deflection associated with the maximum moment, $Area_2$ was used instead of $Area_1$. In this model, the beam was deemed to have failed if the concrete strain was 0.003 or if the CFRP reached its rupture stress.

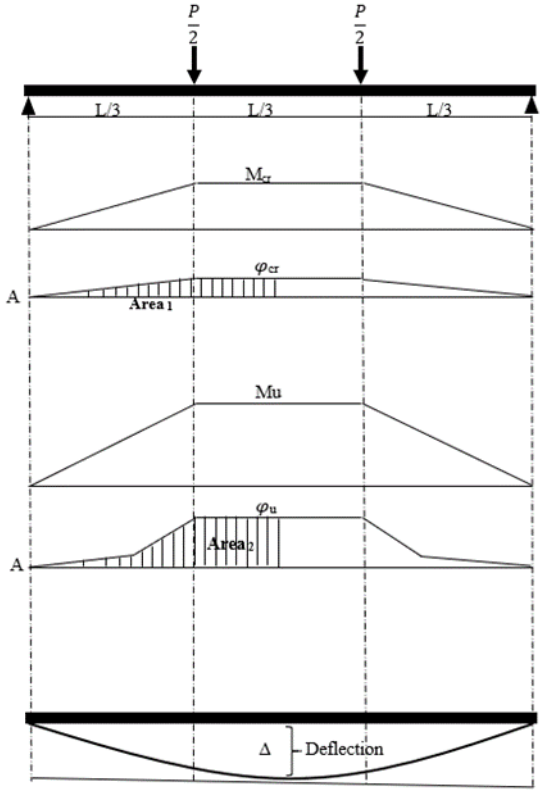

Figure 11. Steps to determine the theoretical mid-span deflection

5.3. Theoretical results and discussions

Figure 12 shows the results of the theoretical model compared to the experimental results. It can be seen that the theoretical moment-deflection curves are also a bilinear relationship. The moment-deflection curve labeled "Model" in Fig. 12 has two marked failure points. The first one represents the predicted flexural capacity of the beam when CFRP material reached the ultimate guaranteed tensile capacity (2070 MPa). The second marked point, which was always higher than the first point, represent the predicted flexural capacity of the beam when CFRP materials reached the actual ultimate tensile capacity or when the concrete ultimate strain at the top fiber reached 0.003. Figure 12 shows that the theoretical model for the first three beams predicted a higher flexural capacity with a higher moment-deflection stiffness. This was mainly attributed to the perfect bonding assumption for the theoretical model.

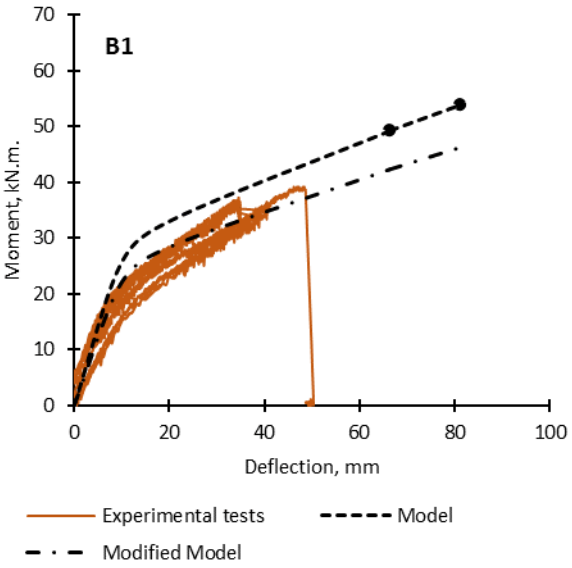

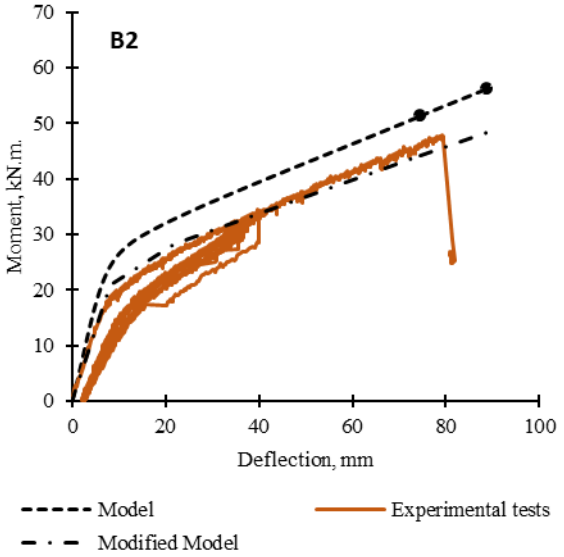

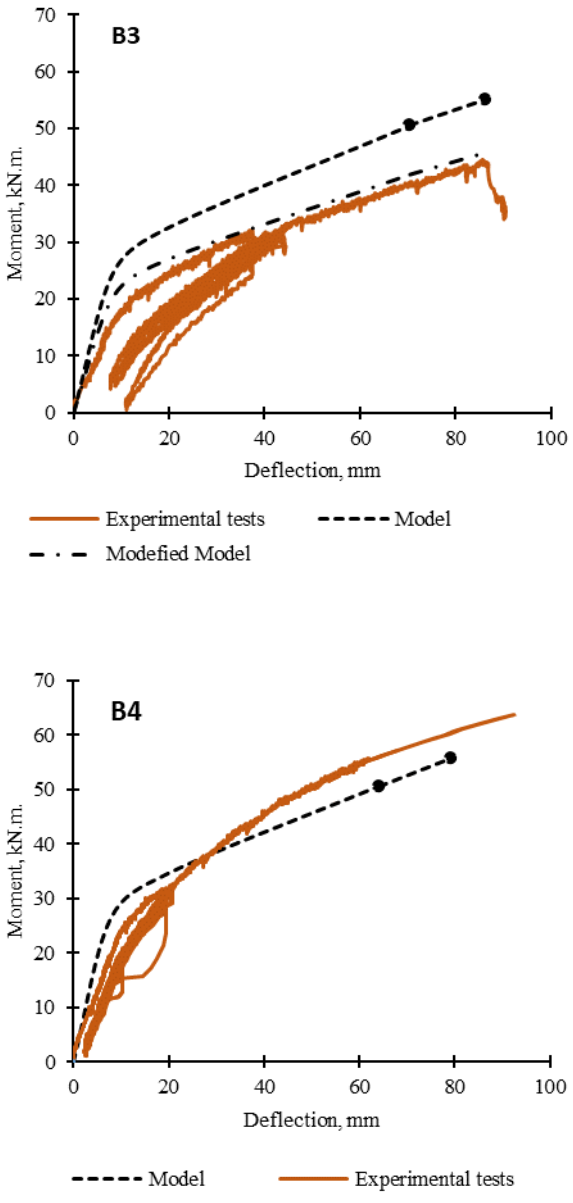

Figure 12. Moment-deflection curves; experimental vs. theoretical prediction (***continued***)

The main cause of failure for the first three beam specimens was CFRP slippage, which also caused a lower flexural stiffness and sudden failure in the shear span (for B1 and B2). In addition, the beam specimens were subjected to five cycles of loading and unloading before the monotonic test, while the theoretical model did not account for the first 5 cycles of loading. This would also reduce the flexural stiffness of the beams, especially the first part of the curves.

The results of B4 led to more confidence in terms of the above observations. When CFRP rods were locked at the beam ends (slippage ~ zero), the flexural moment capacity and the moment deflection stiffness improved significantly, and the theoretical prediction became much closer to the experimental tests. Therefore, it is expected that if the experimental tests for the first beams repeated with anchoring CFRP rods at the beam ends, the prediction would be in a better agreement with the experimental results. Moreover, it can be seen from Fig. 12 that the model reasonably predicted the moment-deflection relationship except the fact that the experimental specimens failed earlier than the expected load due to slippage issue.

5.4. Proposed slippage reduction factor, R_S

In order to have a more accurate theoretical model, it is recommended to account for FRP slippage at the beam ends for FRP prestressed concrete beams [40–42]. This was clear based on the results of the current study. Therefore, it is recommended to investigate the effects of FRP slippage on the performance of FRP prestressed concrete beams and propose an equation or a solution to account for the slippage effects. In the current study, a reduction factor called "R_S" was proposed to accurately predict the moment deflection relationship for CFRP prestressed concrete beams to be used by engineers and researchers until a more comprehensive study is conducted to propose a better model. Based on the results of this study, a reduction factor of 15% (R_S =0.85) seems to be reasonable as shown in Fig 12. The moment-deflection curve labeled "Modified Model" represent the proposed theoretical model with the proposed reduction factor. It can be noticed that the proposed reduction factor significantly improved the prediction of the model, and the theoretical results became in a very good agreement with the experimental results. For B4, a reduction factor or 1 should be used because the CFRP rod was locked at the beam ends. Therefore, no CFRP slippage was expected.

6. Conclusions

Four CFRP prestressed concrete beams were fabricated and tested to investigate the flexural capacity of prestressed concrete beams pre-tensioned with one CFRP rod. A theoretical model was developed, and the results of which were compared to the experimental results. Based on the results of the current study, the following conclusions can be drawn:

1. The minimum shear reinforcement based on ACI 318 is not adequate for prestressed concrete beams pre-tensioned with CFRP rods due to CFRP slippage at the beam ends. Increasing the confinement can improve the bond between CFRP rods and concrete.
2. Locking CFRP rods at the ends prevented CFRP slippages and significantly improved the flexural capacity or performance of prestressed concrete beams.
3. The theoretical model proposed in this study can reasonably predict the flexural response of CFRP prestressed concrete beams. However, a more accurate model would account for CFRP slippage and the effects of cyclic loading on the flexural response of CFRP prestressed concrete beams.
4. The proposed slippage reduction factor of 15% (R_S =0.85) improved the results of the theoretical model, and it is recommended to be used until a comprehensive analytical or numerical model is developed.
5. The results presented in this study are limited to the parameters used in the experimental program and to the assumption made for the theoretical model. Further research is needed to verify the results and to investigate a wider range of parameters.

Authors' contribution

To be filled later; after the Double-blind peer review process.

Declaration of competing interest

The authors declare no conflicts of interest.

Funding source

The experimental work was funded by the Higher Committee for Education Development in Iraq (HCED).

Data availability

The data that support the findings of this study are available from the corresponding author upon reasonable request.

Acknowledgments

The authors express their gratitude to the Higher Committee for Education Development in Iraq (HCED) for financially supporting the research project, Portland State University for providing laboratory and technical support, the University of Portland for testing materials, colleagues who assisted with laboratory work, and Tom Bennett for his technical support in the laboratory.

REFERENCES

[1] Barros J a. O, Taheri M, Salehian H, Mendes PJD. A design model for fibre reinforced concrete beams pre-stressed with steel and FRP bars. Compos Struct 2012;94:2494–512. doi:10.1016/j.compstruct.2012.03.007.

[2] Noël M, Soudki K. Effect of Prestressing on the Performance of GFRP-Reinforced Concrete Slab Bridge Strips 2013:188–96.

[3] Saeed YM, Aules WA, Rad FN. Flexural strengthening of RC columns with EB-CFRP sheets and NSM-CFRP rods and ropes. Compos Struct 2022;301:116236. doi:10.1016/j.compstruct.2022.116236.

[4] Nanni A. Flexural Behavior and Design of RC Members Using FRP Reinforcement. J Struct Eng 1993;119:3344–59. doi:10.1061/(ASCE)0733-9445(1993)119:11(3344).

[5] Hollaway LC. A review of the present and future utilisation of FRP composites in the civil infrastructure with reference to their important in-service properties. Constr Build Mater 2010;24:2419–45. doi:10.1016/j.conbuildmat.2010.04.062.

[6] Benmokrane B, Chaallal O, Masmoudi R. Flexural Response of Concrete Beams Reinforced withFRP Reinforcing Bars. Struct J 1996;93:46–55. doi:10.14359/9839.

[7] Yost JR, Gross SP, Dinehart DW. Effective Moment of Inertia for Glass Fiber-Reinforced Polymer-Reinforced Concrete Beams. Struct J 2003;100:732–9. doi:10.14359/12839.

[8] Sonobe Y, Fukuyama H, Okamoto T, Kani N, Kimura K, Kobayashi K, et al. Design Guidelines of FRP Reinforced Concrete Building Structures. J Compos Constr 1997;1:90–115. doi:10.1061/(ASCE)1090-0268(1997)1:3(90).

[9] Nanni A. Fiber-reinforced-plastic (FRP) reinforcement for concrete structures : properties and applications 1993:450.

[10] Burningham CA, Pantelides CP, Reaveley LD. New unibody clamp anchors for posttensioning carbon-fiber-reinforced polymer rods. PCI J 2014;59:103–13.

[11] Saeed YM, Rad FN. Experimental investigation of CFRP prestressed concrete beams. Am. Concr. Institute, ACI Spec. Publ., vol. 2017- March, 2017.

[12] Zhang B, Benmokrane B, Chennouf A, Mukhopadhyaya P, El-safty A. Tensile behavior of Frp tendons for prestressed ground anchors. J Compos Constr 2001;5:85–93. doi:10.1061/(ASCE)1090-0268(2001)5:2(85).

[13] Grace NF, Jensen E, Matsagar V, Penjendra P. Performance of an AASHTO Beam Bridge Prestressed with CFRP Tendons. J Bridg Eng 2013;18:110–21. doi:10.1061/(ASCE)BE.1943-5592.0000339.

[14] Al-Mayah A, Soudki KA, Plumtree A. Experimental and analytical investigation of a stainless steel anchorage for CFRP prestressing tendons. PCI J 2001;46:88–100. doi:10.15554/pcij.03012001.88.100.

[15] Sayed-Ahmed E, Shrive NG. A new steel anchorage system for post-tensioning applications using carbon fibre reinforced plastic tendons. Can J Civ Eng 1998;25:113–27. doi:10.1139/l97-054.

[16] Saadatmanesh H, Ehsani MR. RC Beams Strengthened with GFRP Plates. I: Experimental Study. J Struct Eng 1991;117:3417–33. doi:10.1061/(ASCE)0733-9445(1991)117:11(3417).

[17] Malek AM, Saadatmanesh H. Analytical Study of Reinforced Concrete Beams Strengthened with Web-Bonded Fiber Reinforced Plastic Plates or Fabrics. Struct J 1998;95:343–52. doi:10.14359/551.

[18] Braimah A, Green MF, Soudki KA. Long-Term Behavior of CFRP Prestressed Concrete Beams. PCI J 2003;48:98–107.

[19] Peng F, Xue W. Analytical Approach for Flexural Capacity of FRP Prestressed Concrete T-Beams with Non-Prestressed Steel Bars. J Compos Constr 2018;22:04018063. doi:10.1061/(ASCE)CC.1943-5614.0000903.

[20] Cao Q, Zhou J, Wu Z, Ma ZJ. Flexural behavior of prestressed CFRP reinforced concrete beams by two different tensioning methods. Eng Struct 2019;189:411–22. doi:10.1016/J.ENGSTRUCT.2019.03.051.

[21] Zou PXW, Shang S. Time-dependent behaviour of concrete beams pretensioned by carbon fibre-reinforced polymers (CFRP) tendons. Constr Build Mater 2007;21:777–88. doi:10.1016/J.CONBUILDMAT.2006.06.008.

[22] Garg S, Matsagar V, Marburg S. Nonlinear Finite Element Analyses of Prestressed Concrete Beams Strengthened with CFRP Laminate. Struct Eng Int 2023;33:258–64. doi:10.1080/10168664.2022.2158449.

[23] ASTM Standard D7205/D7205M. Standard Test Method for Tensile Properties of Fiber Reinforced Polymer Matrix Composite Bars. West Conshohocken, PA: ASTM International; 2011.

[24] ASTM C469/ C469 - 10. Standard Test Method for Static Modulus of Elasticity and Poisson's Ratio of Concrete in Compression. 2010.

[25] ACI Committee 440 (ACI 440.1R-15). Guide for the Design and Construction of Structural Concrete Reinforced with Fiber-Reinforced Polymer Bars. Farmington Hills, MI.: 2015.

[26] ACI Committee 318 (ACI 318-19). Building Code Requirements for Structural Concrete and Commentary. Farmington Hills, MI.: 2019.

[27] Nanni A, Tanigaki M. Pretensioned Prestressed Concrete Memberswith Bonded Fiber Reinforced Plastic Tendons:Development and Flexural Bond Lengths (Static). Struct J 1992;89:433–41. doi:10.14359/9640.

[28] Harajli M, Abouniaj M. Bond Performance of GFRP Bars in Tension: Experimental Evaluation and Assessment of ACI 440 Guidelines. J Compos Constr 2010;14:659–68. doi:10.1061/(ASCE)CC.1943-5614.0000139.

[29] Mahmoud Z, Rizkalla SH, E Z. Transfer and Development Lengths of Carbon Fiber Reinforced Polymers Prestressing Reinforcement. ACI Struct J 1999;96.

[30] Saeed YM, Al-Obaidi SM, Al-hasany EG, Rad FN. Evaluation of a new bond-type anchorage system with expansive grout for a single FRP rod. Constr Build Mater 2020;261:120004. doi:10.1016/j.conbuildmat.2020.120004.

[31] ACI Committee 440 (ACI 440R-07). ACI PRC-440-07 Report on Fiber-Reinforced Polymer (FRP) Reinforcement for Concrete Structures. 2007.

[32] Abdelrahman AA, Tadros G, Rizkalla SH. Test Model for the First Canadian Smart Highway Bridge. ACI Struct J 1995;92:451–8.

[33] Zou PXW. Flexural behavior and deformability of fiber reinforced polymer prestressed concrete beams. J Compos Constr 2003;7:275–84.

[34] Nawy EG. Prestressed Concrete: A Fundamental Approach. Fifth. Prentice Hall; 2009.

[35] Wee TH, Chin MS, Mansur M a. Stress-Strain Relationship of High-Strength Concrete in Compression. J Mater Civ Eng 1996;8:70–6.

[36] ACI Committee 440 (ACI 440.4R-04). Prestressing Concrete Structures with FRP Tendons. Farmington Hills, MI.: 2004.

[37] Bank LC. Composites for construction: structural design with FRP materials. New Jersey, USA: John Wiley & Sons Inc.; 2006.

[38] Zoghi M. The international handbook of FRP Composites in Civil

Engineering. Boca Raton, FL: Taylor & Francis Group, LLC; 2014.
[39] The MathWorks Inc. MATLAB version: 9.13.0 (R2022b) 2017.
[40] Saeed YM. Behavior of Prestressed Concrete Beams with CFRP Strands. Portland State University, 2016. doi:10.15760/etd.2722.
[41] Yao LZ, Wu G. Fiber-element modeling for seismic performance of square RC bridge columns retrofitted with NSM BFRP bars and/or BFRP sheet confinement. J Compos Constr 2016;20:1–15. doi:10.1061/(ASCE)CC.1943-5614.0000652.
[42] El Refai A. Durability and fatigue of basalt fiber-reinforced polymer bars gripped with steel wedge anchors. J Compos Constr 2013;17. doi:10.1061/(ASCE)CC.1943-5614.0000417.